NJC

PAPER

View Article Online
View Journal | View Issue

Two novel indolo[3,2-*b*]carbazole derivatives containing dimesitylboron moieties: synthesis, photoluminescent and electroluminescent properties†

Cite this: *New J. Chem.*, 2014, **38**, 2368

Heping Shi,*[ab] Jiandong Yuan,[a] Xiaohuan Wu,[a] Xiuqing Dong,[c] Li Fang,[a] Yanqin Miao,[d] Hua Wang*[d] and Fangqin Cheng*[c]

Received (in Montpellier, France) 28th January 2014,
Accepted 21st February 2014

DOI: 10.1039/c4nj00140k

www.rsc.org/njc

Two novel indolo[3,2-*b*]carbazole derivatives, 5,11-di(4′-dimesitylboronphenyl)indolo[3,2-*b*]carbazole (**DDBICZ**) and 2,8-dimesitylboron-5,11-di(4′-dimesitylboronphenyl)indolo[3,2-*b*]carbazole (**DDDBICZ**), were synthesized by introducing two dimesitylboron groups and/or four dimesitylboron groups (as electron-acceptors) into the indolo[3,2-*b*]carbazole moiety (as an electron-donor). The structures of these two compounds were fully characterized by elemental analysis, mass spectrometry and proton nuclear magnetic resonance spectroscopy methods. Their thermal properties were studied by thermogravimetric analysis and differential scanning calorimetry. Their electrochemical and photophysical properties were studied by electrochemical methods, UV-vis absorption spectroscopy and fluorescence spectroscopy. The charge-transporting properties of **DDBICZ** and **DDDBICZ** were studied by fabricating single carrier devices using them as charge-transporting layers. The results reveal that **DDBICZ** and **DDDBICZ** have high thermal stability (the decomposition temperature of **DDBICZ** = 201 °C and the decomposition temperature of **DDDBICZ** = 210 °C) and good electrochemical and electron-transporting properties. Moreover, in order to examine the electroluminescent properties of **DDBICZ** and **DDDBICZ**, **Device A** and **Device B** were fabricated by using them as light-emitting layers, respectively. The turn-on voltage, maximum luminance and maximum luminance efficiency of **Device A** are 6.1 V, 5634 cd m^{-2} and 2.96 cd A^{-1}, whereas those of **Device B** are 3.6 V, 1363 cd m^{-2} and 2.88 cd A^{-1}.

1. Introduction

Since the seminal work on organic light-emitting diodes (OLEDs) by Tang and VanSlyke,[1] organic electroluminescent (EL) devices have gained enormous attention owing to their promising applications in solid-state lighting and full-color flat-panel display devices.[2–7] With the purpose of improving the efficiency and stability of the OLEDs, many efforts have been made to develop various novel organic materials with desirable properties.[8–10] Among these high-performance materials, indolo[3,2-*b*]carbazole (ICZ) derivatives and boron-containing π-conjugated compounds are the popular ones due to their excellent performance in EL devices.

Indolo[3,2-*b*]carbazole (ICZ) derivatives have received much attention due to their large planar and rigid conjugated structures together with their remarkable photophysical properties. Many ICZ derivatives with outstanding properties such as better morphological stability and thermal durability as well as desirable charge-injecting and transporting properties have been reported during the past few decades. Ong and his co-workers reported a series of ICZ derivatives, which could serve as excellent hole-transporting materials and organic thin-film transistor (OTFT) materials.[11–14] Tao *et al.* designed and synthesized several ICZ derivatives, which can be used as excellent luminescence and hole-transporting materials in the OLEDs.[15–17] Boudreault *et al.* synthesized some new materials based on the ICZ framework, which were particularly suitable for organic field-effect transistors (OFETs).[18,19] Grazulevicius and his co-workers developed various *N*,*N*-diarylated ICZ derivatives and these compounds can serve as hole-transporting materials for

---

[a] *School of Chemistry and Chemical Engineering, Shanxi University, 92 Wucheng Road, Taiyuan 030006, Shanxi Province, China. E-mail: hepingshi@sxu.edu.cn; Fax: +86-351-7011688; Tel: +86-351-7010588*
[b] *State Key Laboratory of Luminescent Materials and Devices, South China University of Technology, Guangzhou, Guangdong, 510640, PR China*
[c] *State Environmental Protection Key Laboratory of Efficient Utilization Technology of Coal Waste Resources, Shanxi University, 92 Wucheng Road, Taiyuan 030006, Shanxi Province, China. E-mail: cfangqin@sxu.edu.cn; Fax: +86-351-7018813; Tel: +86-351-7018813*
[d] *Key Laboratory of Interface Science and Engineering in Advanced Materials, Taiyuan University of Technology, Taiyuan 030024, Shanxi Province, China. E-mail: wanghua001@tyut.edu.cn*

† Electronic supplementary information (ESI) available. See DOI: 10.1039/c4nj00140k

OLEDs.[20–24] Recently, Chen *et al.* reported two new ICZ derivatives with multifunctionality, which were employed as deep-blue emitters, hole-transporting materials and hosts to fabricate organic light-emitting devices.[25]

Boron-containing π-conjugated compounds have emerged during the past decade. They have high fluorescence quantum yields owing to the overlap between the vacant p-orbital of the boron center and the conjugated moieties,[26–34] which make these compounds a promising class of candidates for optoelectronic materials. Generally, for the application of organoboron compounds in optoelectronic materials and devices, the boron center must resist nucleophilic attack and hydrolysis. Researchers have readily achieved this by functionalizing the boron center with bulky aryl substituents.[35] Thus, triarylboron compounds containing a dimesitylboron group and/or several dimesitylboron groups have been successfully developed as materials for nonlinear optics[36,37] and anion sensing[38–47] and utilized as emitting and/or electron-transporting materials for OLEDs.[48–57] Shirota and co-workers first reported the use of triarylboranes in OLEDs. They designed and synthesized a series of emitting materials with desired bipolar character containing a dimesitylboron group.[50,51] Inspired by the work done by Shirota's group, Wang and co-workers synthesized various donor–acceptor type triarylboranes as blue emitting materials, including compounds based on BNPB,[54,55] DPA and AZAIN systems.[53,58] They evaluated the performances of those compounds by fabricating EL devices. Their results showed that BNPB-2 can act as either a bifunctional electron-transporting and blue-emitting material in a simple double-layer EL device or a trifunctional electron-transporting, hole-transporting and blue-emitting material in a triple-layer EL device,[54] BNPB-5 can act as an excellent hole-transporting material in OLEDs,[28] and BDPA-2 and BDPA-3 can be used as both blue-emitting and electron-transporting materials in OLEDs.[53] In addition, they investigated the use of triarylboron-containing metal complexes as phosphorescent materials in OLEDs.[59–63] Besides Wang and co-workers, many other research groups have devoted great efforts to explore triarylborane compounds for use in OLEDs. Among them, Lambert and co-workers synthesized a series of amino-substituted triarylboranes (TABs) and investigated their electrochemical and photophysical properties.[64] Later, they synthesized polymers based on the carbazole-substituted TABs mentioned above.[65] They found that the 3,6-linked polycarbazole is a promising candidate for application in OLEDs. Despite all those efforts made by different groups, the field of boron-containing optoelectronic materials still remains largely unexplored.

As mentioned above, compounds containing the ICZ moiety and/or the dimesitylboron moiety are attractive materials for the organic electroluminescent (EL) devices due to their efficient luminescence and transport performance. Thus we became interested in incorporating the ICZ moiety and the dimesitylboron moiety into a single molecule to obtain novel materials with excellent luminescent, hole-transporting and electron-transporting properties.

In this paper, two new ICZ derivatives, 5,11-di(4′-dimesitylboronphenyl)indolo[3,2-*b*]carbazole (**DDBICZ**) and 2,8-dimesitylboron-5,11-di(4′-dimesitylboronphenyl)indolo[3,2-*b*]carbazole (**DDDBICZ**), were synthesized by introducing dimesitylboron groups into the ICZ moiety. The synthetic route is presented in Scheme 1. To the best of our knowledge, these compounds have never been reported before. The structures of **DDBICZ** and

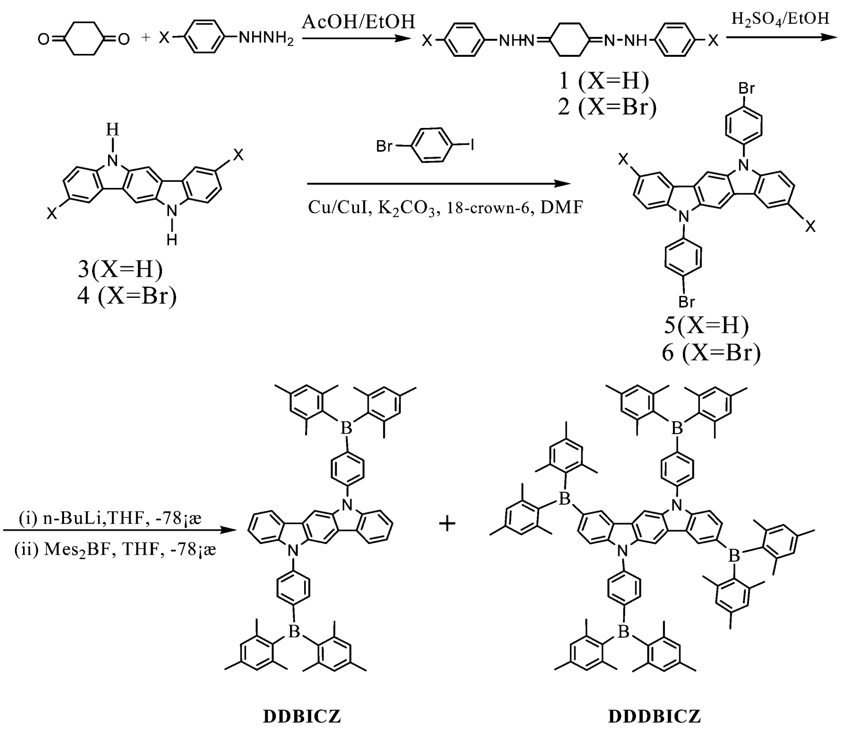

Scheme 1 The synthetic routes for preparation of **DDBICZ** and **DDDBICZ**.

DDDBICZ were characterized by ^{1}H NMR, ^{13}C NMR, MS and elemental analysis. The thermal, electrochemical, photoluminescent properties were determined by thermogravimetric analysis combined with electrochemistry, UV-vis absorption spectroscopy and fluorescence spectroscopy. Furthermore, the electroluminescent properties were characterized by the devices fabricated using these compounds.

2. Experimental

2.1. Synthesis of compounds

The synthesis of compounds cyclohexane-1,4-dione-diphenyl hydrazone (**1**), cyclohexane-1,4-dione-bis(*p*-bromophenyl)-hydrazone (**2**), indolo[3,2-*b*]carbazole (**3**) and 2,8-dibromoindolo[3,2-*b*]carbazole (**4**) was performed according to or slightly modified literature procedures.[66]

2.1.1 Synthesis of cyclohexane-1,4-dione-diphenyl hydrazone (compound 1). To a solution of 1,4-cyclohexanedione (5 g, 44.5 mmol) in absolute EtOH (100 mL) were added 90 mL of absolute ethyl alcohol and 0.1 mL of acetic acid. The reaction mixture was stirred for 20 min, and then 10.73 mL of phenylhydrazine was added dropwise. The reaction mixture was heated to 35 °C and kept at the same temperature for 30 min and then cooled. The precipitate was slowly filtered off, washed carefully with water and dried to give cyclohexane-1,4-dione-diphenyl hydrazone (7.13, 54.9%) as a yellow powder.

2.1.2 Synthesis of cyclohexane-1,4-dione-bis(*p*-bromophenyl)-hydrazone (compound 2). 1,4-Cyclohexanedione (5.62 g, 50 mmol) was dissolved in absolute ethanol (EtOH) (100 mL) and was added with stirring to a mixture of powdered 4-bromophenylhydrazine hydrochloride (22.4 g, 100 mmol), sodium acetate (8.2 g, 100 mmol) and absolute ethanol (200 mL) at room temperature. The mixture was quickly heated to 50 °C, and then the temperature was cooled to 0 °C. The precipitate was filtered off and washed carefully with water to give **2** (yield 59%).

2.1.3. Synthesis of indolo[3,2-*b*]carbazole (compound 3). Cyclohexane-1,4-dione-bisphenyl hydrazone (10 g, 0.036 mmol) was added portionwise to a mixture of AcOH and H_2SO_4 (4 : 1, 50 mL) with stirring at 10 °C. Thereafter, the mixture was heated to 30 °C and kept for 30 min. Afterwards, the temperature was increased slowly to 60–70 °C and the mixture changed colour from bright raspberry to grey-green. After half an hour, the reaction mixture was refluxed for another 30 min with the colour changing to yellow. Then the mixture was allowed to cool to room temperature and the precipitate was slowly filtered off and was washed carefully with water and EtOH, and dried to give the target compound (5.74 g, 62.3%) as a yellow solid.

2.1.4. Synthesis of 2,8-dibromoindolo[3,2-*b*]carbazole (compound 4). Compound **2** (10 g, 22 mmol) was added into a mixture of AcOH (130 mL) and H_2SO_4 (32 mL) at 0 °C and stirred for 5 min. The mixture was heated up to 30 °C and kept stirring for 1 h. Afterward, the temperature of the mixture was further increased up to 60–70 °C and stirred for another 1 h. Then it was cooled down to room temperature and poured into ice water with stirring. The greenish solid was filtered off and washed with water and EtOH to neutral pH. Finally, dry and pure 2,8-dibromoindolo[3,2-*b*]carbazole (compound **4**) (4.88 g, yield 52.8%) was achieved. Mp > 300 °C, ^{1}H NMR (600 MHz DMSO-d$_6$) δ (ppm): 11.14 (2H, s, and N–H) and 7.1–8.24 (8H, m, and Ar–H).

2.1.5. Synthesis of 5,11-di(4′-bromophenyl)indolo[3,2-*b*]-carbazole (compound 5). Indolo[3,2-*b*]carbazole (2.563 g, 10 mmol) and 1-bromo-4-iodobenzene (8.487 g, 30 mmol) were dissolved in 80 mL of dry DMF under a nitrogen atmosphere. Then powdered potassium carbonate (11.040 g, 80 mmol), Cu (2.921 g, 46 mmol) and 18-crown-6 (1.056 g, 4 mmol) were added into it. The mixture was stirred for 30 min at room temperature and then heated up slowly to 150 °C and kept for 48 h. Afterwards, the reaction mixture was cooled down to room temperature and poured into ice water with stirring 1 h. The precipitate was collected and recrystallized with EtOH and dried finally. The residue was purified by flash chromatography on silica gel (CH_2Cl_2/hexane) to afford compound **5**. Yield: 50%, Mp: >300 °C, ^{1}H NMR (600 MHz $CDCl_3$) δ (ppm): 8.118 (2H, d, *J* = 7.8), 8.033–7.992 (3H, m, *J* = 7.2), 7.805 (3H, d, *J* = 8.4), 7.575 (3H, d, *J* = 8.4), 7.359–7.384 (5H, m, *J* = 9.0), 7.273 (1H, d, *J* = 7.2), 6.981 (1H, s).

2.1.6 Synthesis of 2,8-dibromo-5,11-di(4′-bromophenyl)indolo-[3,2-*b*]carbazole (compound 6). To a solution of 2,8-dibromoindolo-[3,2-*b*]carbazole (2.76 g, 6.7 mmol) in anhydrous DMF (80 mL) in the round-bottomed flask, 1-bromo-4-iodobenzene (5.64 g, 20 mmol) was added under a nitrogen atmosphere. Then powdered potassium carbonate (7.36 g, 53 mmol), CuI (0.38 g, 2 mmol) and 18-crown-6 (0.704 g, 2.7 mmol) were added into it. The mixture was heated up slowly to 170 °C after stirring for 30 min at room temperature and kept for 48 h. Then, the reaction mixture was cooled down to room temperature and poured into ice water with stirring for 1 h. The precipitate was collected and recrystallized with EtOH and dried. The crude product was purified by flash chromatography on silica gel (CH_2Cl_2/hexane) to afford compound **6**. Yield: 28.7%, Mp: >300 °C, ^{1}H NMR (600 MHz $CDCl_3$) δ (ppm): 8.674 (1H, s), 8.375–8.363 (2H, t, *J* = 4.2), 8.074 (1H, d, *J* = 7.8), 7.918 (2H, d, *J* = 7.8), 7.714 (4H, t, *J* = 7.8), 7.606–7.513 (3H, m, *J* = 7.8), 7.349 (2H, d, *J* = 9.0), 7.240 (1H, d, *J* = 9.0).

2.1.7. Synthesis of 5,11-di(4′-dimesitylboronphenyl)indolo-[3,2-*b*]carbazole (DDBICZ). Compound **5** (0.846 g, 1.5 mmol) was suspended in anhydrous THF (60 mL) under a nitrogen atmosphere and the solution was cooled to −78 °C with stirring. To this solution, butyllithium (1.7 mL, 2.2 M in hexanes) was injected and the resulting solution was stirred for 30 min at this temperature. Afterwards, the reaction solution was raised to room temperature and kept so for 6 h. Then the solution was cooled to −78 °C again and dimesitylboron fluoride (1.005 g, 3.75 mmol) was quickly added into the stirred reaction mixture under a nitrogen atmosphere. The mixture was allowed to warm to room temperature with stirring for 48 h. Afterwards, the solvent was removed. The residue was diluted with CH_2Cl_2 and the organic layer was collected. The combined organic phase was evaporated *in vacuo* and the residue was washed carefully with Et_2O and EtOH, filtered off and dried to get the crude product, and the crude product was purified by flash chromatography on silica gel (CH_2Cl_2/hexane) to obtain **DDBICZ** (0.464 g, 34%) as a light yellow solid. ^1H NMR (600 MHz $CDCl_3$) δ (ppm): 8.146 (4H, dd, J = 19.8, 22.2), 7.815 (4H, d, J = 7.8), 7.700 (4H, d, J = 4.2), 7.527 (2H, d, J = 4.2), 7.415 (4H, t, J = 7.2), 6.892 (8H, s), 2.345 (12H, s), 2.150 (24H, s). ^{13}C NMR (600 MHz $CDCl_3$) δ (ppm): 144.612, 144.521, 144.480, 143.787, 141.773, 141.081, 139.551, 132.900, 132.793, 130.239, 130.018, 129.050, 128.983, 128.904, 128.800, 126.797, 126.672, 123.211, 123.159, 123.107, 122.707, 122.657, 122.611, 122.100, 112.690, 112.644, 103.106, 102.973, 102.888, 26.454, 24.119. MS (*m*/*z*): 904.6 (M+). Anal. Calcd for $C_{66}H_{62}B_2N_2$: C, 87.61%; H, 6.91%; N, 3.10%. Found: C, 87.69%; H, 6.87%; N, 3.14%.

2.1.8 Synthesis of 2,8-dimesitylboron-5,11-di(4′-dimesitylboronphenyl)indolo[3,2-*b*]carbazole (DDDBICZ). Compound 6 (0.5 g, 0.69 mmol) was dissolved in anhydrous THF (60 mL) under a nitrogen atmosphere and the resulting solution was cooled to −78 °C with stirring. Then, *n*-butyllithium (5.3 mL, 1.3 M in hexanes) was added to the stirred solution at this temperature. After 30 min, the reaction solution was raised to room temperature and kept so for 6 h. Then, the solution was cooled to −78 °C again and dimesitylboron fluoride (2.22 g, 8.28 mmol) was quickly added into the stirred reaction mixture under a nitrogen atmosphere. The mixture was allowed to warm to room temperature with stirring for 48 h. Afterwards, the solvent was evaporated and the residue was extracted with water and CH_2Cl_2. The organic layer was collected and evaporated *in vacuo*, and then the residue was washed carefully with Et_2O and EtOH, filtered off and dried to get the crude product. Finally, the crude product was purified by flash chromatography on silica gel (CH_2Cl_2/hexane) to obtain **DDDBICZ** (0.268 g, 28%) as a light yellow solid. ^1H NMR (600 MHz DMSO) δ (ppm): 8.335 (2H, s), 8.068 (2H, s), 7.802 (4H, d, J = 7.8), 7.651 (4H, d, J = 8.4), 7.589 (2H, d, J = 8.4), 7.368 (2H, d, J = 8.4), 6.874 (8H, s), 6.842 (8H, s), 2.346 (12H, s), 2.327 (12H, s), 2.104 (24H, s), 2.049 (24H, s). ^{13}C NMR (600 MHz DMSO) δ (ppm): 145.15, 144.533, 143.847, 143.795, 143.725, 141.759, 141.227, 141.045, 140.184, 138.772, 133.096, 132.766, 131.982, 131.213, 131.035, 130.427, 129.231, 127.019, 126.571, 112.056, 103.872, 32.563, 28.493, 26.489, 26.405, 24.095. MS (*m*/*z*): 1401.5 (M+). Anal. Calcd for $C_{102}H_{104}B_4N_2$: C, 87.43%; H, 7.48%; N, 2.00%. Found: C, 87.37%; H, 7.51%; N, 2.05%.

2.2 Measurement and characterization

Melting points were determined using an X-5 melting point detector. All NMR spectra were recorded on a Bruker 600 MHz spectrometer. Thermogravimetric analysis (TGA) was performed using a TGA 2050 thermogravimetric analyser under a N_2 atmosphere with a heating rate of 10 °C min^{-1} from room temperature to 750 °C. Differential scanning calorimetry (DSC) was performed using a Q2000 DSC differential scanning calorimeter under a N_2 atmosphere with a heating rate of 10 °C min^{-1} from room temperature to 250 °C. Elemental analyses were performed using an Element Analysis System. Mass spectra were recorded using a LC-MS system consisting of a Waters 1525 pump and a Micromass ZQ4000 single quadrupole mass spectrometer detector. Cyclic voltammetry (CV) was performed using a CHI-600C electrochemical analyser. The CV measurements were carried out with a conventional three-electrode configuration consisting of a glassy carbon working electrode, a platinum-disk auxiliary electrode and a Ag/AgCl reference electrode, and the scan speed was 50 mV s^{-1}. UV-vis absorption spectra were acquired using a Shimadzu UV-2450 spectrophotometer. Fluorescence spectra were obtained using a Hitachi F-4500 spectrofluorometer. Fluorescence quantum yield was determined by using quinine sulfate as the reference. All measurements were performed at room temperature.

2.3 Device fabrication and testing

The multilayer OLEDs were fabricated by the vacuum-deposition method. Organic layers were deposited by high-vacuum (5 × 10^{-4} Pa) thermal evaporation onto a glass (3 cm × 4 cm) substrate pre-coated with an indium tin oxide (ITO) layer. *N*,*N*-bis(naphthyl)-*N*,*N*-bis(phenyl)benzidine (NPB), 4,4-cyclohexylidene-bis[*N*,*N*-bis-(4-methylphenyl)benzenamine] (TAPC), **DDBICZ**/**DDDBICZ**, 2,9-dimethyl-4,7-diphenyl-1,10-phenanthroline (BCP), 4,7-diphenyl-1,10-phenanthroline (BPhen) and LiF/Al were used as the hole-transporting layer, electron-blocking layer, emitting layer, hole-blocking layer, electron-transporting layer and cathode, respectively. All organic layers were sequentially deposited. Thermal deposition rates for organic materials, LiF and Al were 0.5, 0.5 and 1 Å s^{-1}, respectively. The active area of the devices was 12 mm^2. The electroluminescent spectra were measured using a Hitachi MPF-4 spectrofluorometer. The voltage–current density (*V*–*J*) characteristics of OLEDs were recorded using a Keithley 2400 Source Meter. The characterization of brightness–current–voltage (*B*–*I*–*V*) were measured with a 3645 DC power supply combined with a 1980A spot photometer and were recorded simultaneously. All measurements were done at room temperature under ambient conditions.

2.4. Theoretical calculations

The ground-state geometries of **DDBICZ** and **DDDBICZ** were optimized at the B3LYP level with the 6-31G(d,p) basis set.[67–69] Their vibration frequencies and frontier molecular orbital characteristics were analysed on the optimized structure at the same level. Solvent effect was also taken into account by using the polarised continuum model.[70,71] All calculations were carried out using the Gaussian 03 program package[72] and performed in the Supercomputing Centre of Computer Network Information Centre of the Chinese Academy of Sciences.

3. Results and discussion

3.1 Synthesis

As shown in Scheme 1, the syntheses of indolo[3,2-*b*]carbazole derivatives comprising dimesitylboron moieties were carried out using a multi-step synthetic route. Firstly, compound **1** was synthesized *via* the reaction of 1,4-cyclohexanedione with phenylhydrazine. Then compound **3** was prepared by the Fischer reaction of compound **1** in a mixture of acetic acid and sulfuric acid at 65 °C in high yield. Secondly, the intermediate compound

5 was prepared by the reaction of indolo[3,2-*b*]carbazole with 1-bromo-4-iodobenzene in the presence of Cu, 18-crown-6 and potassium carbonate at 170 °C with 50% yield. Finally, **DDBICZ** was synthesized by the reaction of compound **5** with *n*-BuLi and dimesitylboron fluoride at −78 °C with 34% yield. The synthetic route for preparation of **DDDBICZ** was similar to that of **DDBICZ**. **DDDBICZ** was obtained in 28% yield. **DDBICZ** and **DDDBICZ** were characterized by ^{1}H NMR, ^{13}C NMR, MS and elemental analysis. The ^{1}H NMR spectra of **DDBICZ** and **DDDBICZ** displayed downfield peaks at 7.00–8.48 ppm, which were assigned to the protons of the 5,11-diphenylindolo[3,2-*b*]carbazole moiety. The downfield peaks at 6.59–6.89 ppm and the upfield peaks at 2.09 and 2.37 ppm were assigned to the protons of dimesitylboron moieties. The ^{13}C NMR, mass spectrometry and elemental analysis were consistent with the desired structures. Further details are given in the Experimental section. **DDBICZ** and **DDDBICZ** are soluble in many common organic solvents such as dichloromethane, chloroform, DMF, THF, toluene and DMSO.

3.2 Thermal properties

The thermal properties of **DDBICZ** and **DDDBICZ** were investigated by thermogravimetric analysis (TGA) and differential scanning calorimetry (DSC) under a nitrogen atmosphere. The TGA and DSC curves of **DDBICZ** and **DDDBICZ** are shown in Fig. 1 and 2, respectively. The decomposition temperatures (T_d) were observed for **DDBICZ** (T_d = 201 °C) and **DDDBICZ** (T_d = 210 °C) by TGA analyses. The glass transition temperatures (T_g) were observed for **DDBICZ** (T_g = 145 °C) and **DDDBICZ** (T_g = 162 °C) by DSC analyses. These data are also collected in Table 1. The high T_d and T_g of **DDBICZ** and **DDDBICZ** can be attributed to their large molecular mass, rigid indolo[3,2-*b*]carbazole cores and non-planar dimesitylboron peripheries. Our results indicate that these two compounds have excellent thermal properties which should be adequate for most optoelectronic device applications.

3.3 Theoretical calculations

Theoretical calculations can provide a reasonable qualitative indication of the excitation and emission properties of a compound.[73] The ground-state geometries of **DDBICZ** and **DDDBICZ** were optimized at the B3LYP level with the 6-31G(d,p) basis set. The vibration frequencies and the frontier molecular orbital characteristics were analyzed on the optimized structures at the same level. The molecular structure of **DDBICZ** contains a 5,11-diphenylindolo[3,2-*b*]carbazole unit as the core and two dimesitylboron groups as the terminals. As shown in Fig. 3, the

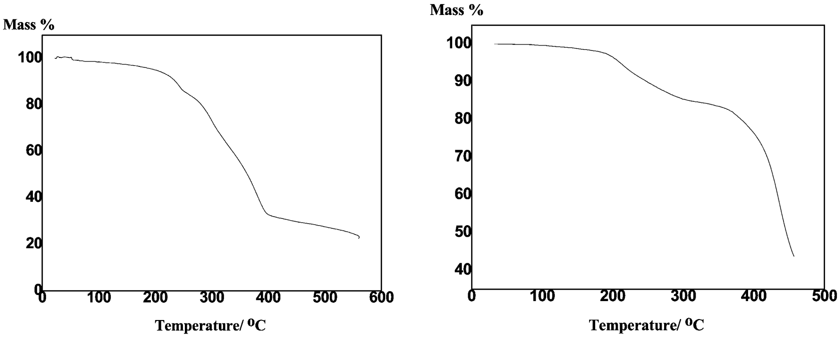

(a) TGA curve of **DDBICZ** (b) TGA curve of **DDDBICZ**

Fig. 1 TGA curves of **DDBICZ** and **DDDBICZ**.

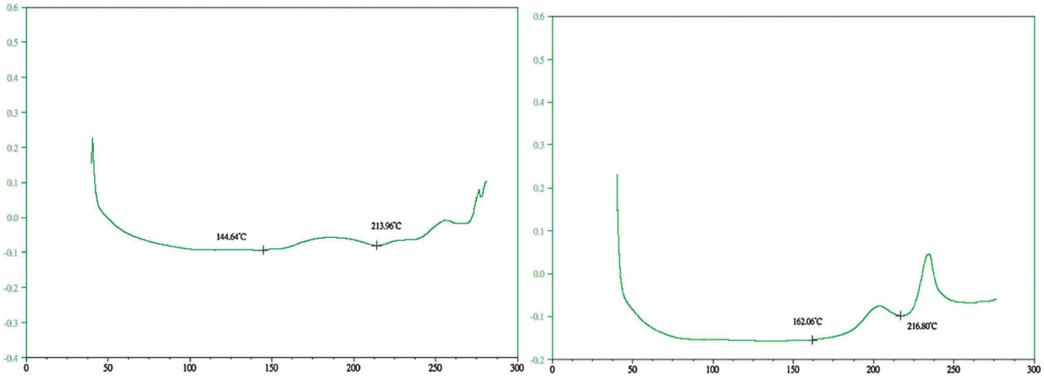

(a) DSC curve of **DDBICZ** (b) DSC curve of **DDDBICZ**

Fig. 2 DSC curves of **DDBICZ** and **DDDBICZ**.

Table 1 Physical properties of compounds **DDBICZ** and **DDDBICZ**

				HOMO (eV)		LUMO (eV)		E_g (eV)			
Compounds	λ_{abs} (nm)	λ_{em} (nm)	Φ	Theo	Exp	Theo	Exp	Theo	Exp	T_d (°C)	T_g (°C)
DDBICZ	337	474	0.52							201	145
	398			−5.20	−5.27	−1.97	−2.38	3.23	2.89		
DDDBICZ	345	453	0.48							210	162
	382			−5.34	−5.28	−2.02	−2.32	3.32	2.96		

λ_{abs}, absorption peak maximum; λ_{em}, emission peak maximum in film; Φ, fluorescent quantum yield in THF; HOMO: highest occupied molecular orbital; LUMO: lowest unoccupied molecular orbital; E_g, energy gap between HOMO and LUMO; T_d, decomposition temperature; T_g, glass transition temperature

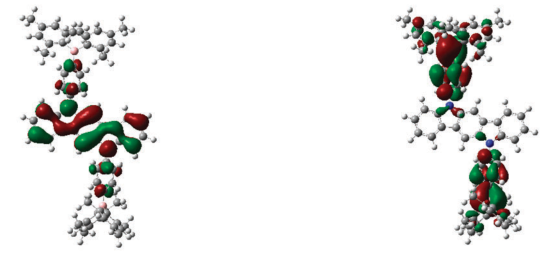

(a)HOMO of **DDBICZ** (a) LUMO of **DDBICZ**

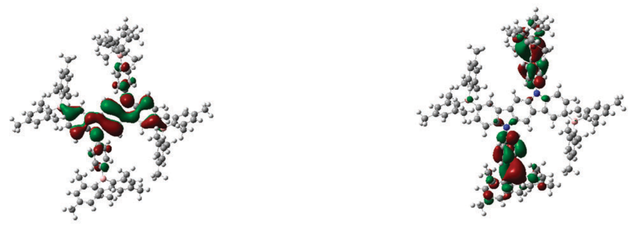

(b) HOMO of **DDDBICZ** (b) LUMO of **DDDBICZ**

Fig. 3 HOMO and LUMO diagrams of **DDBICZ** and **DDDBICZ**.

indolo[3,2-*b*]carbazole moiety has planar structure, the two phenyl groups present a twisted structure relative to this plane and the two mesityl groups form propeller-like conformations originating from the trigonal boron center. The highest occupied molecular orbital (HOMO) and the lowest unoccupied molecular orbital (LUMO) of **DDBICZ** were also calculated at the DFT/B3LYP/6-31G(d,p) level using the polarized continuum model for geometry optimization. Coordinates of **DDBICZ** are collected in Table S1 (ESI†). The HOMO of **DDBICZ** is localized mainly in the indolo[3,2-*b*]carbazole moiety, while the LUMO is localized in the dimesitylborylphenyl moiety (Fig. 1a). The molecular structure of **DDDBICZ** contains a 5,11-diphenylindolo[3,2-*b*]carbazole unit as the core and four dimesitylboron groups as the terminals. The geometry of **DDDBICZ** at the ground state was optimized using the same method. Coordinates of **DDDBICZ** are collected in Table S2 (ESI†). Fig. 1b shows that the geometry of **DDDBICZ** is similar to **DDBICZ** and the distributions of the HOMO and the LUMO of **DDDBICZ** are similar to those of **DDBICZ**, respectively. Generally, holes and electrons in OLEDs are transferred through the individual HOMO and LUMO levels.[74] Fig. 1a and b show that **DDBICZ** and **DDDBICZ** exhibit almost complete separation of LUMO and HOMO, which is essential for the efficient hole and electron transport.[75] The calculated HOMO and LUMO energy levels and the energy gap of **DDBICZ** are −5.20, −1.97 and 3.23 eV (Table 1), while those of **DDDBICZ** are −5.34, −2.02 eV and 3.32 eV (Table 1), respectively. The theoretical HOMO and LUMO levels of **DDBICZ** and **DDDBICZ** are higher than the experimental ones, the HOMO–LUMO energy gaps of **DDBICZ** and **DDDBICZ** in theory are *ca.* 0.34 eV and 0.36 eV larger than those of the optical energy bands obtained from UV-vis absorption measurements, respectively.

3.4 Photophysical properties

Fig. 4a shows the absorption spectra of **DDBICZ** in various solvents (1.0×10^{-5} M). The absorption spectra data are summarized in Table 1. As depicted in Fig. 4a, **DDBICZ** exhibits two major absorption bands at 290–350 and 350–429 nm, respectively. The absorption peak maximum (λ_{abs}) of 337 nm corresponds to the π–π* electronic transition of the indolo[3,2-*b*]-carbazole skeleton and the λ_{abs} of 398 nm corresponds to intramolecular charge transfer (ICT) from the indolo[3,2-*b*]carbazole core to dimesitylboron terminals. Fig. 4b shows the absorption spectra of **DDDBICZ** in various solvents (1.0×10^{-5} M). The absorption spectra data are also summarized in Table 1. As shown in Fig. 4b, the absorption spectra of **DDDBICZ** are similar to those of **DDBICZ** in various solvents. The optical energy band gap of **DDBICZ** calculated from the absorption band edge of the absorption spectrum is approximately 2.89 eV, while that of **DDDBICZ** is approximately 2.96 eV. The normalized fluorescence spectra of **DDBICZ** in various solvents (1.0×10^{-5} M) are shown in Fig. 5a and the data are also collected in Table 1. As shown in Fig. 5a, **DDBICZ** exhibits strong fluorescence emission bands at 390–670 nm in various solvents. The emission peak maximums (λ_{em}) exhibit a red-shift of 115 nm ranging from 425 nm (in hexane) to 540 nm (in DMSO) with the increasing polarity of the solvents, which is assigned to π–π* transition of the intramolecular charge transfer (ICT) from the indolo[3,2-*b*]carbazole core to the dimesitylboron terminals in the excitation process. The fluorescence spectra of **DDDBICZ** show similar characteristics to those of **DDBICZ** in various solvents (Fig. 5b). The emission bands are located at 390–660 nm with a red-shift of 95 nm ranging from 423 nm (in hexane) to 518 nm (in DMSO). The fluorescence quantum yields (Φ) of **DDBICZ** and **DDDBICZ** in several solvents (1.0×10^{-6} M) were measured by using quinine bisulfate in 0.10 M sulfuric acid as the reference[76] and collected in Table 1.

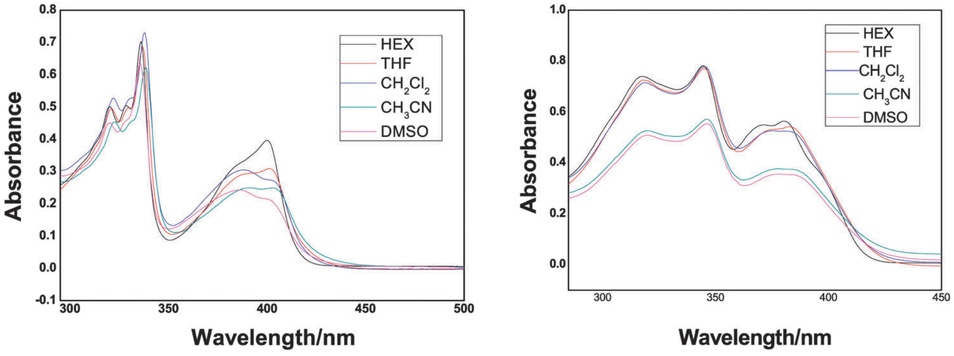

(a) (b)

Fig. 4 The UV-vis absorption spectra of **DDBICZ** and **DDDBICZ** in several solvents.

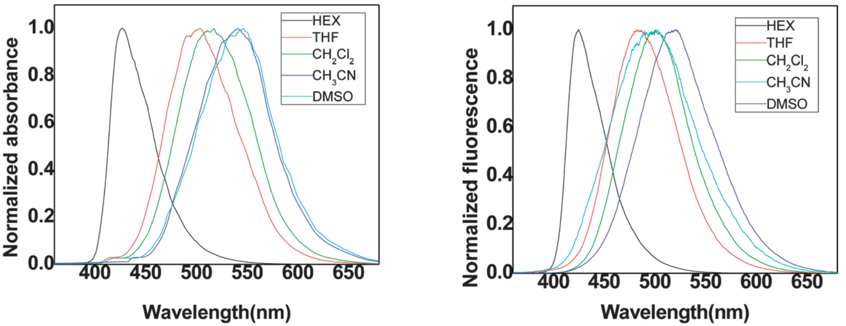

(a) (b)

Fig. 5 The normalized fluorescence spectra of **DDBICZ** and **DDDBICZ** in several solvents.

As shown in Table 1, **DDBICZ** and **DDDBICZ** have relatively high fluorescence quantum yields, revealing their potential application as excellent optoelectronic materials in the optical field.

3.5 Electrochemical properties

The electrochemical properties of **DDBICZ** and **DDDBICZ** were studied by cyclic voltammetry (CV) with Ag/AgCl as the reference electrode. The measurement was conducted in 1.0 mM **DDBICZ** and/or **DDDBICZ** in acetonitrile containing 0.10 M tetrabutylammonium perchlorate as the supporting electrolyte under N_2 atmosphere. The CVs of **DDBICZ** are displayed in Fig. 6a. As shown in Fig. 6a, a reversible oxidation peak and one reversible reduction peak are observed within the entire electrochemical window of acetonitrile. The reversible oxidation peak at around +1.12 V is assigned to the oxidation of indolo[3,2-*b*]carbazole, whereas the reversible reduction peak at around −1.23 V is attributed to the electron injection into the vacant p-orbital of dimesitylboron. The CVs of **DDDBICZ** are displayed in Fig. 6b. As shown in Fig. 6b, its reversible oxidation and reduction peak is at +1.18 V and −1.25 V, respectively. The electrochemical behaviors of **DDDBICZ** are similar to those of **DDBICZ**. The HOMO energy level can be calculated with the empirical equation: HOMO = $-(E_{\text{ox}} + 4.40)$ eV, where E_{ox} is the onset oxidation potential.[77] The E_{ox} of **DDBICZ** is 0.87 and the HOMO

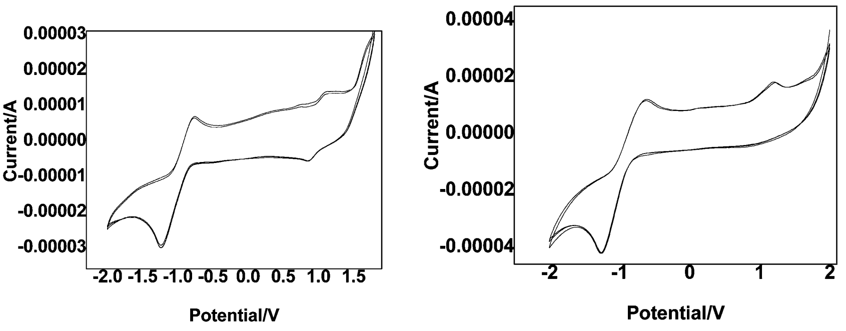

(a) (b)

Fig. 6 The cyclic voltammogram curves of **DDBICZ** and **DDDBICZ**.

energy level of **DDBICZ** is −5.27 eV. The E_g is estimated to be 2.89 eV by the absorption edge of the absorption spectrum of **DDBICZ**. The LUMO energy level of **DDBICZ** is thus −2.38 eV which is calculated from the HOMO energy level and E_g. The HOMO, LUMO and E_g of **DDBICZ** are very close to the theoretical values (Table 1). Similar to **DDBICZ**, the HOMO, LUMO and E_g of **DDDBICZ** are also very close to the theoretical values (Table 1). The LUMO levels of **DDBICZ** and **DDDBICZ** are as low as those of two common electron-transporting materials, 1,3,5-tris(1-phenyl-1*H*-benzimidazol-2-yl)benzene (2.39 eV) and 2,9-dimethyl-4,7-diphenyl-1,10-phenanthroline (**BCP**) (2.44 eV), indicating that these two compounds have small barrier of electron transport and can be used as effective electron-transporting materials for OLEDs.[78] Furthermore, the CV curves of the compounds remained unchanged under multiple successive potential scans, indicating that the compounds have excellent redox properties.[79]

3.6 Charge-transporting properties

In order to further demonstrate the charge-transporting properties of **DDBICZ** and **DDDBICZ**, several single carrier devices were prepared. First, two hole-only devices, ITO/TAPC (8 nm)/**DDBICZ** (30 nm)/TAPC (8 nm)/Al and ITO/TAPC (8 nm)/**DDDBICZ** (30 nm)/TAPC (8 nm)/Al, were prepared to examine the hole-transporting capability of **DDBICZ** and **DDDBICZ**, respectively. In which TAPC was used to block the electron from the cathode because of its high LUMO level. Then, another two electron-only devices, ITO/BCP (8 nm)/**DDBICZ** (30 nm)/BCP (8 nm)/LiF (1 nm)/Al and ITO/BCP (8 nm)/**DDDBICZ** (30 nm)/BCP (8 nm)/LiF (1 nm)/Al, were prepared to examine the electron-transporting capability of **DDBICZ** and **DDDBICZ**, respectively. In which BCP was used to block the hole from the anode because of its low HOMO level. Fig. 7 depicts the current-characteristics of the four devices as a function of the average electric field. Both devices fabricated by using **DDBICZ** can conduct rather significant currents, suggesting that **DDBICZ** has hole- and electron-transporting capabilities. Under the same average electric field, the electron-only device conducts higher currents than the hole-only device, indicating that **DDBICZ** may possess stronger electron-transporting ability despite its bipolar capability (Fig. 7a). The devices based on **DDDBICZ** show similar performance to the devices fabricated by using **DDBICZ** (Fig. 7b). Our results are in good agreement with the results obtained by Lin *et al.*[80] Thus, these two compounds are promising candidates as electron-transporting materials.

3.7 Electroluminescent properties

In order to evaluate **DDBICZ** and/or **DDDBICZ** as potential luminescent materials for their application in OLEDs, two multilayer organic electroluminescence (EL) devices with the configuration of ITO/NPB (50 nm)/**DDBICZ** (50 nm)/Bphen (20 nm)/LiF (0.5 nm)/A1 (**Device A**) and ITO/NPB (50 nm)/**DDDBICZ** (50 nm)/Bphen (20 nm)/LiF (0.5 nm)/A1 (**Device B**) were fabricated, where NPB and Bphen were used as the hole-transporting layer and the electron-transporting layer, respectively. The EL spectra of **Device A** measured at different voltages are shown in Fig. S1 (ESI†), which are in good agreement with those of **DDBICZ** films. (The PL spectra of **DDBICZ** films are displayed in Fig. S2 (ESI†).) The EL spectra of **Device A** exhibit the same pure blue emissions at different voltages with a maximum at 472 nm and CIE coordinates of $x = 0.22$ and $y = 0.32$. The current density–voltage–luminance curves of **Device A** are shown in Fig. 8a and the luminance efficiency–current density curve of **Device A** is shown in Fig. 8b. The electroluminescent data for **Device A** are summarized in Table 2. As shown in Table 2, the turn-on voltage, maximum luminance and maximum luminance efficiency of **Device A** are 6.1 V, 5634 cd m^{-2} and 2.96 cd A^{-1}, respectively. The EL spectra of **Device B** measured at different voltages are shown in Fig. S3 (ESI†), which are in good agreement with those of **DDDBICZ** films. (The PL spectra of **DDDBICZ** films are displayed in Fig. S4 (ESI†).) The EL spectra of **Device B** exhibit the same pure blue emissions at different voltages with a maximum at 464 nm and CIE coordinates of $x = 0.16$ and $y = 0.19$. The current density–voltage–luminance curves of **Device B** are shown in Fig. 9a and the luminance efficiency–current density curve for **Device B** is shown in Fig. 9b. The electroluminescent data for **Device B** are also summarized in Table 2. As shown in Table 2, the turn-on voltage, maximum luminance and maximum luminance efficiency of **Device B** are 3.6 V, 1363 cd m^{-2} and 2.88 cd A^{-1}, respectively. Although the maximum luminance and luminance efficiency of the EL devices of **DDBICZ** and **DDDBICZ** might not be as high as in some of the blue EL devices reported

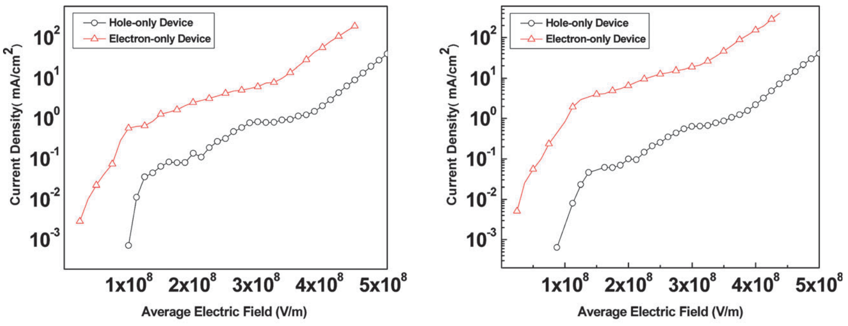

(a) (b)

Fig. 7 The current characteristics as a function of the average electric field for hole-only and electron-only devices of **DDBICZ** and **DDDBICZ**.

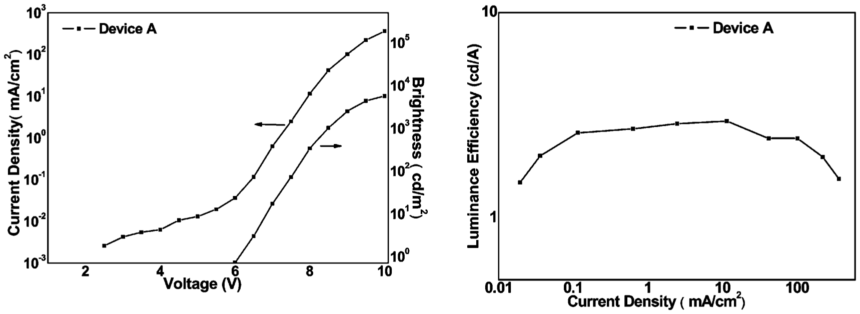

(a) (b)

Fig. 8 Current density–voltage–luminance curves and current density–luminance efficiency curve of **Device A**.

Table 2 Electroluminescent characteristics of **Devices A** and **B**

Devices	λ_{EL} (nm)	V_{on}	L_{max} (cd m^{-2}) (at voltage)	$\eta_{L,max}$ (cd A^{-1}) (at voltage)
A	472	6.1	5634 (at 10 V)	2.96 (at 8 V)
B	464	3.6	1363 (at 10.5 V)	2.88 (at 5.1 V)

λ_{EL}, electroluminescence emission peak; V_{on}, turn-on voltage at 1 cd m^{-2}; L_{max}, maximum luminance; $\eta_{L,max}$, maximum luminance efficiency.

before,[28,51,53,54,81] these two novel compounds are promising for application in OLEDs as emitting materials due to their excellent thermal, electrochemical and charge-transporting properties. In addition, these two materials can be utilized to make white OLED devices by integrating with other materials, and we have obtained some preliminary results. The further large-scale application study of these two materials is currently in progress.

4. Conclusion

In summary, two novel indolo[3,2-*b*]carbazole derivatives, 5,11-di(4′-dimesitylboronphenyl)indolo[3,2-*b*]carbazole (**DDBICZ**) and 2,8-dimesitylboron-5,11-di(4′-dimesitylboronphenyl)indolo[3,2-*b*]-carbazole (**DDDBICZ**) were synthesized by introducing two dimesitylboron groups and/or four dimesitylboron groups (as electron-acceptors) into the indolo[3,2-*b*]carbazole moiety (as electron-donor). The structures of these two compounds were fully characterized by elemental analysis, mass spectrometry and proton nuclear magnetic resonance spectroscopy methods. Their thermal, electrochemical and photophysical properties were studied by thermogravimetric analysis combined with differential scanning calorimetry, electrochemistry, UV-vis absorption spectroscopy and fluorescence spectroscopy. The charge-transporting properties of **DDBICZ** and **DDDBICZ** were studied by fabricating single carrier devices using them as charge-transporting layers. The results reveal that **DDBICZ** and **DDDBICZ** have high thermal stability (the decomposition temperature of **DDBICZ** = 201 °C and the decomposition temperature of **DDDBICZ** = 210 °C) and good electrochemical and electron-transporting properties. Moreover, in order to examine the electroluminescent properties of **DDBICZ** and **DDDBICZ**, **Device A** and **Device B** were fabricated by using them as light-emitting layers, respectively. The turn-on voltage, maximum luminance and maximum luminance efficiency of **Device A** are 6.1 V, 5634 cd m^{-2} and 2.96 cd A^{-1}, whereas those of **Device B** are 3.6 V, 2036 cd m^{-2} and 2.88 cd A^{-1}. Our work demonstrates that **DDBICZ** and **DDDBICZ** are promising blue emitting materials with potential application in producing OLED devices.

Acknowledgements

This work was supported by the Natural Science Foundation of Shanxi Province (2013011013-1); Open Fund of the State Key Laboratory of Luminescent Materials and Devices, South China

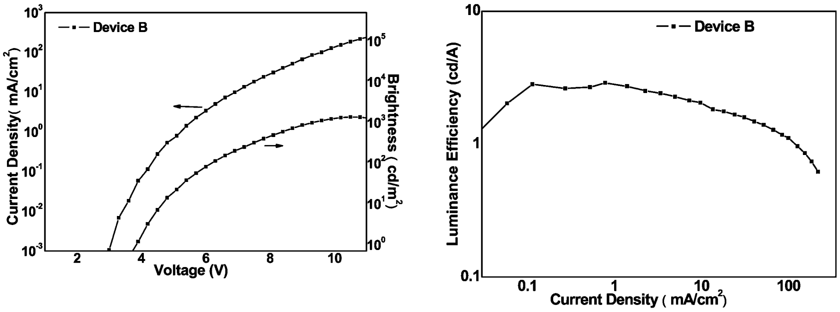

(a) (b)

Fig. 9 Current density–voltage–luminance curves and current density–luminance efficiency curve of **Device B**.

University of Technology (2014-skllmd-09); Scientific and Technological Innovation Programs of Higher Education Institutions in Shanxi Province (2012005); Program for Changjiang Scholar and Innovation Research Team in University (IRT0972); International Science & Technology Cooperation Program of China (2012-DFR50460); National Natural Scientific Foundation of China (21101111, 61205179, 61307030, 61307029, and 21376144); Shanxi Provincial Key Innovative Research Team in Science and Technology (2012041011); Shanxi Scholarship Council of China (2012-006); and Fund of Key Laboratory of Optoelectronic Materials Chemistry and Physics, Chinese Academy of Sciences (2008DP173016). The authors express their sincere thanks to the Advanced Computing Facilities of the Supercomputing Centre of Computer Network Information Centre of Chinese Academy of Sciences for all the theoretical calculations.

References

1 C. W. Tang and S. A. VanSlyke, *Appl. Phys. Lett.*, 1987, **51**, 913–915.

2 M. A. Baldo, D. F. O'Brien, Y. You, A. Shoustikov, S. Sibley, M. E. Thompson and S. R. Forrest, *Nature*, 1998, **395**, 151–154.

3 M. A. Baldo, M. E. Thompson and S. R. Forrest, *Nature*, 2000, **403**, 750–753.

4 X. Gong, D. Moses, A. J. Heeger, S. Liu and A. K. Y. Jen, *Appl. Phys. Lett.*, 2003, **83**, 183–185.

5 Y. Shao and Y. Yang, *Appl. Phys. Lett.*, 2003, **83**, 2453–2455.

6 F. Huang, Y. H. Niu, Y. Zhang, J. W. Ka, M. S. Liu and A. K. Y. Jen, *Adv. Mater.*, 2007, **19**, 2010–2014.

7 Y. Liu, M. Nishiura, Y. Wang and Z. M. Hou, *J. Am. Chem. Soc.*, 2006, **128**, 5592–5593.

8 Q. Zhang, J. Chen, Y. Chen, L. Wang, D. Ma, X. Jing and F. J. Wang, *Mater. Chem.*, 2004, **14**, 895–900.

9 J. Li, C. Ma, J. Tang, C. S. Lee and S. Lee, *Chem. Mater.*, 2005, **17**, 615–619.

10 J. Li, D. Liu, Y. Li, C. S. Lee, H. Kwong and S. Lee, *Chem. Mater.*, 2005, **17**, 1208–1212.

11 N. X. Hu, S. Xie, Z. Popovic, B. S. Ong and A. M. Hor, *J. Am. Chem. Soc.*, 1999, **121**, 5097–5098.

12 Y. L. Wu, Y. N. Li and S. Gardner, *J. Am. Chem. Soc.*, 2005, **127**, 614–618.

13 Y. N. Li, Y. L. Wu, S. Gardner and B. S. Ong, *Adv. Mater.*, 2005, **17**, 849–853.

14 Y. N. Li, Y. L. Wu, S. Gardner and B. S. Ong, *Macromolecules*, 2006, **39**, 6521–6527.

15 H. P. Zhao, X. T. Tao, P. Wang, Y. Ren, J. X. Yang, Y. X. Yan, C. X. Yuan, H. J. Liu, D. C. Zou and M. H. Jiang, *Org. Electron.*, 2007, **8**, 673–682.

16 H. P. Zhao, X. T. Tao, F. Z. Wang, Y. Ren, X. Q. Sun, J. X. Yang, Y. X. Yan, D. C. Zou, X. Zhao and M. H. Jiang, *Chem. Phys. Lett.*, 2007, **439**, 132–137.

17 H. P. Zhao, F. Z. Wang, C. X. Yuan, X. T. Tao, J. L. Sun, D. C. Zou and M. H. Jiang, *Org. Electron.*, 2009, **10**, 925–931.

18 P. T. Boudreault, S. Wakim, M. L. Tang, Y. Tao, Z. Bao and M. Leclerc, *J. Mater. Chem.*, 2009, **19**, 2921–2928.

19 P. T. Boudreault, A. A. Virkar, Z. Bao and M. Leclerc, *Org. Electron.*, 2010, **11**, 1649–1659.

20 M. Kirkus, J. V. Grazulevicius, S. Grigalevicius, R. Gub, W. Dehaen and V. Jankauskas, *Eur. Polym. J.*, 2009, **45**, 410–417.

21 D. Velasco, V. Jankauskas, J. Stumbraite, J. V. Grazulevicius and V. Getautis, *Synth. Met.*, 2009, **159**, 654–658.

22 S. Lengvinaite, J. V. Grazulevicius, S. Grigalevicius, R. Gub, W. Dehaen, V. Jankauskas, B. Zhang and Z. Xie, *Dyes Pigm.*, 2010, **85**, 183–188.

23 M. Kirkus, J. Simokaitiene, J. V. Grazulevicius and V. Jankauskas, *Synth. Met.*, 2010, **160**, 750–755.

24 J. Simokaitiene, E. Stanislovaityte, J. V. Grazulevicius, V. Jankauskas, R. Gu, W. Dehaen, Y. C. Hung and C. P. Hsu, *J. Org. Chem.*, 2012, **77**, 4924–4931.

25 S. Y. Chen, J. B. Wei, K. Wang, C. G. Wang, D. Chen, Y. Liu and Y. Wang, *J. Mater. Chem. C*, 2013, **1**, 6594–6602.

26 C. D. Entwistle and T. B. Marder, *Angew. Chem., Int. Ed.*, 2002, **41**, 2927–2931.

27 C. D. Entwistle and T. B. Marder, *Chem. Mater.*, 2004, **16**, 4574–4585.

28 W. L. Jia, M. J. Moran, Y. Y. Yuan, Z. H. Lu and S. Wang, *J. Mater. Chem.*, 2005, **15**, 3326–3333.

29 J. Wang, F. Q. Bai, B. H. Xia, J. Chen and H. X. Zhang, *J. Organomet. Chem.*, 2011, **696**, 2943–2948.

30 D. X. Cao, Z. Q Liu, G. Z. Li, G. Q. Liu and G. H. Zhang, *J. Mol. Struct.*, 2008, **874**, 46–50.

31 Y. Chen, D. X. Cao, S. S Wang, C. Q. Zhang and Z. Z. Liu, *J. Mol. Struct.*, 2010, **969**, 182–186.

32 V. Zlojutro, Y. Sun and H. S. Wang, *Chem. Commun.*, 2011, **47**, 3837–3839.

33 W. J. Xu, S. J. Liu, T. C. Ma, Q. Zhao, A. Pertegas, D. Tordera, H. J. Bolink, S. H. Ye, X. M. Liu, S. Sun and W. Huang, *J. Mater. Chem.*, 2011, **21**, 13999–14007.

34 M. S. Yuan, Q. Fang, Z. Q. Liu, J. P. Guo, H. Y. Chen, W. T. Yu, G. Xue and D. S. Liu, *J. Org. Chem.*, 2006, **71**, 7858–7861.

35 Z. M. Hudson and S. Wang, *Dalton Trans.*, 2011, **40**, 7805–7816.

36 Z. Yuan, J. C. Collings, N. J. Taylor, T. B. Marder, C. Jardin and J.-F. Halet, *J. Solid State Chem.*, 2000, **154**, 5–12.

37 Z.-Q. Liu, Q. Fang, D. Wang, D.-X. Cao, G. Xue, W.-T. Yu and H. Lei, *Chem.–Eur. J.*, 2003, **9**, 5074–5084.

38 T. W. Hudnall, C. W. Chiu and F. P. Gabbai, *Acc. Chem. Res.*, 2009, **42**, 388–397.

39 Y. Kim and F. P. Gabbai, *J. Am. Chem. Soc.*, 2009, **131**, 3363–3369.

40 C. W. Chiu, Y. Kim and F. P. Gabbai, *J. Am. Chem. Soc.*, 2009, **131**, 60–61.

41 S. Yamaguchi, S. Akiyama and K. Tamao, *J. Am. Chem. Soc.*, 2001, **123**, 11372–17375.

42 S. Yamaguchi and S. Akiyama, *Pure Appl. Chem.*, 2006, **78**, 1413–1424.

43 S. Yamaguchi, T. Shirasaka, S. Akiyama and K. Tamao, *J. Am. Chem. Soc.*, 2002, **124**, 8816–8817.

44 Z.-Q. Liu, M. Shi, F.-Y. Li, Q. Fang, Z.-H. Chen, T. Yi and C. H. Huang, *Org. Lett.*, 2005, **7**, 5481–5484.

45 K. Parab, K. Venkatasubbaiah and F. Jäkle, *J. Am. Chem. Soc.*, 2006, **128**, 12879–12885.

46 F. Jäkle, *Coord. Chem. Rev.*, 2006, **250**, 1107–1121.

47 G. Zhou, M. Baumgarten and K. Müllen, *J. Am. Chem. Soc.*, 2008, **130**, 12477–12484.

48 T. Noda and Y. Shirota, *J. Am. Chem. Soc.*, 1998, **120**, 9714–9715.

49 T. Noda, H. Ogawa and Y. Shirota, *Adv. Mater.*, 1999, **11**, 283–285.

50 Y. Shirota, M. Kinoshita, T. Noda, K. Okumoto and T. Ohara, *J. Am. Chem. Soc.*, 2000, **122**, 11021–11022.

51 H. Doi, M. Kinoshita, K. Okumoto and Y. Shirota, *Chem. Mater.*, 2003, **15**, 1080–1089.

52 Y. Shirota, *J. Mater. Chem.*, 2005, **15**, 75–93.

53 W. L. Jia, D. R. Bai, T. McCormick, Q. D. Liu, M. Motala, R. Wang, C. Seward, Y. Tao and S. Wang, *Chem.–Eur. J.*, 2004, **10**, 994–1006.

54 W. L. Jia, X. D. Feng, D. R. Bai, Z. H. Lu, S. Wang and G. Vamvounis, *Chem. Mater.*, 2005, **17**, 164–170.

55 F. H. Li, W. L. Jia, S. Wang, Y. Q. Zhao and Z. H. Lu, *J. Appl. Phys.*, 2008, **103**, 034509.

56 D. Tanaka, T. Takeda, T. Chiba, S. Watanabe and J. Kido, *Chem. Lett.*, 2007, **36**, 262–263.

57 L. X. Xiao, Z. J. Chen, B. Qu, J. X. Luo, S. Kong, Q. H. Gong and J. Kido, *Adv. Mater.*, 2011, **23**, 926–952.

58 W.-L. Jia, D.-T. Song and S. Wang, *J. Org. Chem.*, 2003, **68**, 701–705.

59 Z. M. Hudson, C. Sun, M. G. Helander, H. Amarne, Z.-H. Lu and S. Wang, *Adv. Funct. Mater.*, 2010, **20**, 3426–3439.

60 Z. M. Hudson, M. G. Helander, Z.-H. Lu and S. Wang, *Chem. Commun.*, 2011, **47**, 755–757.

61 Z. M. Hudson, C. Sun, M. G. Helander, Y.-L. Chang, Z.-H. Lu and S. Wang, *J. Am. Chem. Soc.*, 2012, **134**, 13930–13933.

62 Y.-L. Rao, D. Schoenmakers, Y.-L. Chang, J.-S. Lu, Z.-H. Lu, Y. Kang and S. Wang, *Chem.–Eur. J.*, 2012, **18**, 11306–11316.

63 X. Wang, Y.-L. Chang, J.-S. Lu, T. Zhang, Z.-H. Lu and S. Wang, *Adv. Funct. Mater.*, 2013, DOI: 10.1002/adfm.201302871.

64 R. Stahl, C. Lambert, C. Kaiser, R. Wortmann and R. Jakober, *Chem.–Eur. J.*, 2006, **12**, 2358–2370.

65 D. Reitzenstein and C. Lambert, *Macromolecules*, 2009, **42**, 773–782.

66 L. N. Yudina and J. Bergman, *Tetrahedron*, 2003, **59**, 1265–1275.

67 P. Hohenberg and W. Kohn, *Phys. Rev. B: Condens. Matter Mater. Phys.*, 1964, **136**, 864–871.

68 W. Kohn and L. J. Sham, *Phys. Rev. A: At., Mol., Opt. Phys.*, 1965, **140**, 1133–1138.

69 J. B. Foresman, M. H. Gordon, J. A. Pople and M. J. Frisch, *J. Phys. Chem.*, 1992, **96**, 135–149.

70 M. Cossi, N. Rega, G. Scalmani and V. Barone, *J. Chem. Phys.*, 2001, **114**, 5691–5701.

71 M. Cossi, G. Scalmani, N. Rega and V. Barone, *J. Chem. Phys.*, 2002, **117**, 43–54.

72 M. J. Frisch, G. W. Trucks, H. B. Schlegel, G. E. Scuseria, M. A. Robb, J. R. Cheeseman, J. A. Montgomery Jr, T. Vreven, K. N. Kudin, J. C. Burant, J. M. Millam, S. S. Iyengar, J. Tomasi, V. Barone, B. Mennucci, M. Cossi, G. Scalmani, N. Rega, G. A. Petersson, H. Nakatsuji, M. Hada, M. Ehara, K. Toyota, R. Fukuda, J. Hasegawa, M. Ishida, T. Nakajima, Y. Honda, O. Kitao, H. Nakai, M. Klene, X. Li, J. E. Knox, H. P. Hratchian, J. B. Cross, C. Adamo, J. Jaramillo, R. Gomperts, R. E. Stratmann, O. Yazyev, P. Salvador, J. J. A. J. Austin, R. Cammi, C. Pomelli, J. W. Ochterski, P. Y. Ayala, K. Morokuma, G. A. Voth, P. S. Dannenberg, V. G. Zakrzewski, S. Dapprich, A. D. Daniels, M. C. Strain, O. Farkas, D. K. Malick, A. D. Rabuck, K. Raghavachari, J. B. Foresman, J. V. Ortiz, Q. Cui, A. G. Baboul, S. Clifford, J. Cioslowski, B. B. Stefanov, G. Liu, A. Liashenko, P. Piskorz, I. Komaromi, R. L. Martin, D. J. Fox, T. Keith, M. A. Al-Laham, C. Y. Peng, A. Nanayakkara, M. Challacombe, P. M. W. Gill, B. Johnson, W. Chen, M. W. Wong, C. Gonzalez and J. A. Pople, *GAUSSIAN 03 (Revision B.05)*, Gaussian, Inc., Pittsburgh, PA, 2003.

73 M. Belletete, J. F. Morin, M. Leclerc and G. Durocher, *J. Phys. Chem. A*, 2005, **109**, 6953–6959.

74 J. Y. Jeon, T. J. Park, W. S. Jeon, J. J. Park, J. Jang, J. H. Kwon and J. Y. Lee, *Chem. Lett.*, 2007, **36**, 1156–1157.

75 Z. Ge, T. Hayakawa, S. Ando, M. Ueda, T. Akiike, H. Miyamoto, T. Kajita and M. Kakimoto, *Adv. Funct. Mater.*, 2008, **18**, 584–590.

76 J. N. Dmas and G. A. Crobys, *J. Phys. Chem.*, 1971, **75**, 991–1024.

77 J. L. Brédas, R. Silbey, D. S. Boudreaux and R. R. Chance, *J. Am. Chem. Soc.*, 1983, **105**, 6555–6559.

78 J. Y. Zhuang, W. M. Su, W. F. Li, Y. Y. Zhou, Q. Shen and M. Zhou, *Org. Electron.*, 2012, **13**, 2210–2219.

79 V. Promaraka and S. Ruchirawat, *Tetrahedron*, 2007, **63**, 1602–1609.

80 M.-S. Lin, S.-J. Yang, H.-W. Chang, Y.-H. Huang, Y.-T. Tsai, C.-C. Wu, S.-H. Chou, E. Mondal and K.-T. Wong, *J. Mater. Chem.*, 2012, **22**, 16114–16120.

81 W. G. Zhang, Z. Q. He, Y. S. Wang and S. M. Zhao, *Synth. Met.*, 2011, **161**, 2323–2328.